GSA DATA REPOSITORY 2010281

TEMPORAL VARIATION OF SEISMIC VELOCITY AND ANISOTROPY BEFORE THE 2009 M_W 6.3 L'AQUILA EARTHQUAKE, ITALY

DETAILS ON FORESHOCK LOCALIZATION

The foreshock activity was characterized by clustering of the events around the main shock nucleation area, beginning about 6 months before the April 6th 2009, M_W 6.3, L'Aquila earthquake, and intensifying 3 months before. Starting from January 2009, the INGV national and regional permanent seismic networks recorded more than 300 earthquakes in a 30 km radius area around the L'Aquila town, about 250 of which densely concentrated in the rock volume containing the focus of the main shock. The dense configuration of the seismic network in the epicentral area (eleven 3-components seismic stations within 30 km radius from L'Aquila town) yields a very consistent detection of small earthquakes, allowing for an optimal sampling of the fault volume. To rely only on events with accurate location, we adopt strict selection criteria, which downsize the total number of earthquakes considered to 188 events with magnitude ranging from M_L = 1.0 to M_L = 4.0. Details on the 1-D velocity model adopted to localize the foreshocks are in Table DR1 and Figure DR1.

DIFFERENCES BETWEEN THE POPULATIONS OF V_P/V_S BEFORE AND AFTER MARCH 30th, AND THEIR STATISTICAL SIGNIFICANCE.

Differences in the S - P arrival time of closely located foreshocks, before and after March 30th, demonstrate that observed variation of V_P/V_S are due to changing medium properties along analogous ray-path (Fig. DR2).

To assess the statistical significance of the differences between the populations of V_P/V_S before and after the time of occurrence of the ML = 4 foreshock, on March 30th, we derive the respective 95% confidence intervals for each of the time series shown in Figure 2 of the paper. At this confidence level for three of the four time series (TOT, FIAM, AQU), the V_P/V_S populations are significantly different, because their respective 95% confidence intervals do not overlap each other (Table DR2). The difference between the two V_P/V_S populations at station GSO2 is not statistically significant (Table DR2).

DEPENDENCE OF THE V_P/V_S ESTIMATES ON THE EVENT LOCATION

To make sure that the migration of seismicity is not responsible for an apparent variations of the speed ratio, nor is the 1-D velocity model adopted to localize the foreshocks, we compute the time series of the V_P/V_S values by different methods and different velocity model. We test the iterative procedure by the Hypoellipse code (Lahr, 1980), which solves least square problem for linear regression when errors are on both variables. This method applies the traditional Wadati (1933) approach, for which the earthquake hypocenter parameters are not needed. This approach does not allow the computation of V_P/V_S values at single stations. Furthermore we apply our method of computing V_P/V_S values, using estimates of origin time derived from two different hypocentral location strategies: using a 3-D, P and S waves, velocity model (Fig. DR3A) derived from the tomographic analysis of the L'Aquila earthquake aftershock sequence (Di Stefano et al., in prep); through the standard double difference location code HypoDD (Waldhauser and Ellsworth, 2000) (Fig. DR3B). The V_P/V_S values from these three tests are processed as those shown in the paper and their trends are compared in Figure DR3C. This comparison

evidences that, regardless of the approach used, the sudden increase of the V_P/V_S in the epicenter area on March 30th is a stable feature.

NULL SPLITTING SHEAR-WAVES

Most of the seismograms analyzed do not show shear wave splitting because of AQU position relative to the hypocenters and the prevalent faulting mechanisms. When the initial polarization of the shear wave is parallel to the fast or slow directions of the anisotropic media the S-wave does not split giving a null measurement (Wüstefeld and Bokelmann, 2007). Although nulls do not provide any information on the delay time, they can be used to constrain the orientation of the anisotropy axis (Fig. 3D of the paper). Consistently with theory, the S-wave which show no splitting are linearly polarized just at about 90° from the prevalent observed fast direction (Figs. 3C and 3D of the paper), and undergoes a sharp change through March 30th. Before this date, null directions are about N50E, i.e. 90° from φ = N140E, after that, the null directions show larger scatter and the prevalent value is about N70E, i.e. 90° from φ = N160E (Figs. DR4C and DR4F).

References

Chiarabba, C., et al., 2009, The 2009 L'Aquila (central Italy) MW 6.3 earthquake: Main shock and aftershocks: Geophys. Res. Lett., v. 36, L18308, doi:10.1029/2009GL039627.

Lahr, J.C., 1980, HYPOELLIPSE: A computer program for determining local earthquake hypocentral parameters, magnitude and first motion patterns: U.S. Geological Survey Open-File Report 79-43.

Wadati, K., 1933, On the travel time of earthquake waves. Part II: Geophys. Mag., v. 7, p. 101–111.

Waldhauser, F., and Ellsworth, W.L., 2000, A double-difference earthquake location algorithm: Method and application to the Northern Hayward Fault, California: Bull. Seism. Soc. Am., v. 90, p. 1353–1368.

Wüstefeld, A, and Bokelmann, G., 2007, Null detection in shear-wave splitting measurements: Bull. Seism. Soc. Am., v. 97, p. 1204–1211.

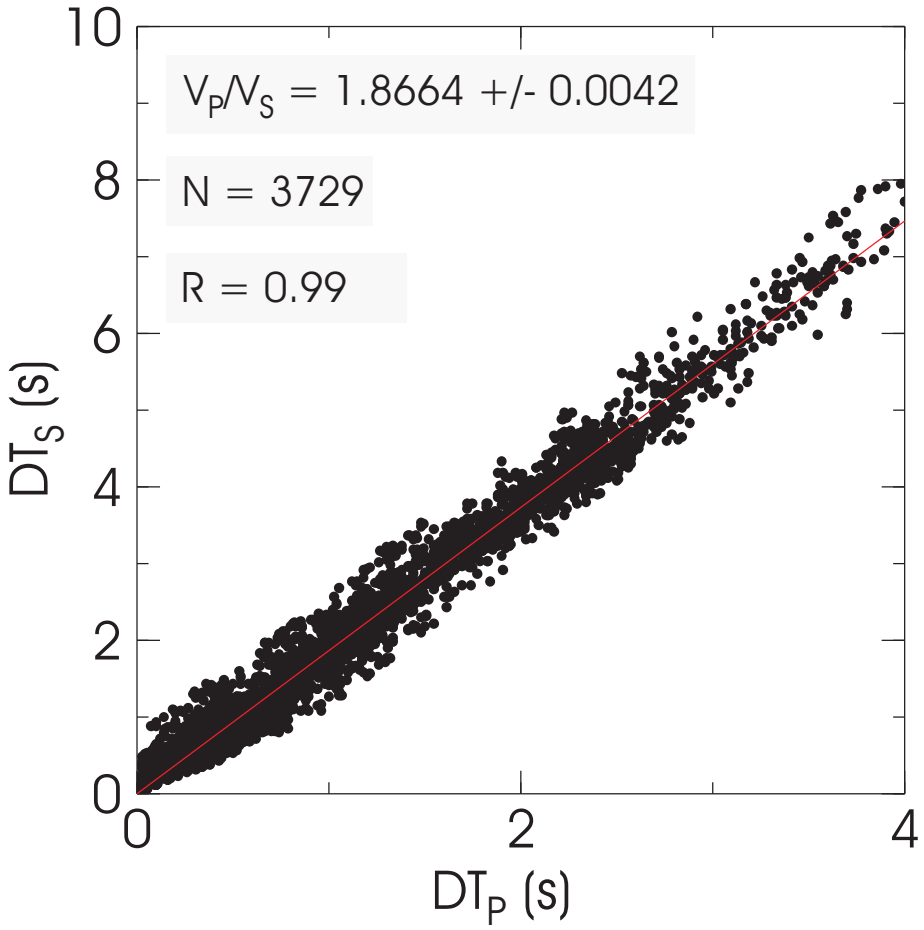

Figure DR1. Wadati (1933) diagram computed on all the earthquakes occurred within 30 km radius from L'Aquila town from September 2008. For each event, DTP and DTS are the differences between P- and S-phases arrival times, respectively, at couple of stations. N is the number of measurements. R is the correlation coefficient of the linear regression.

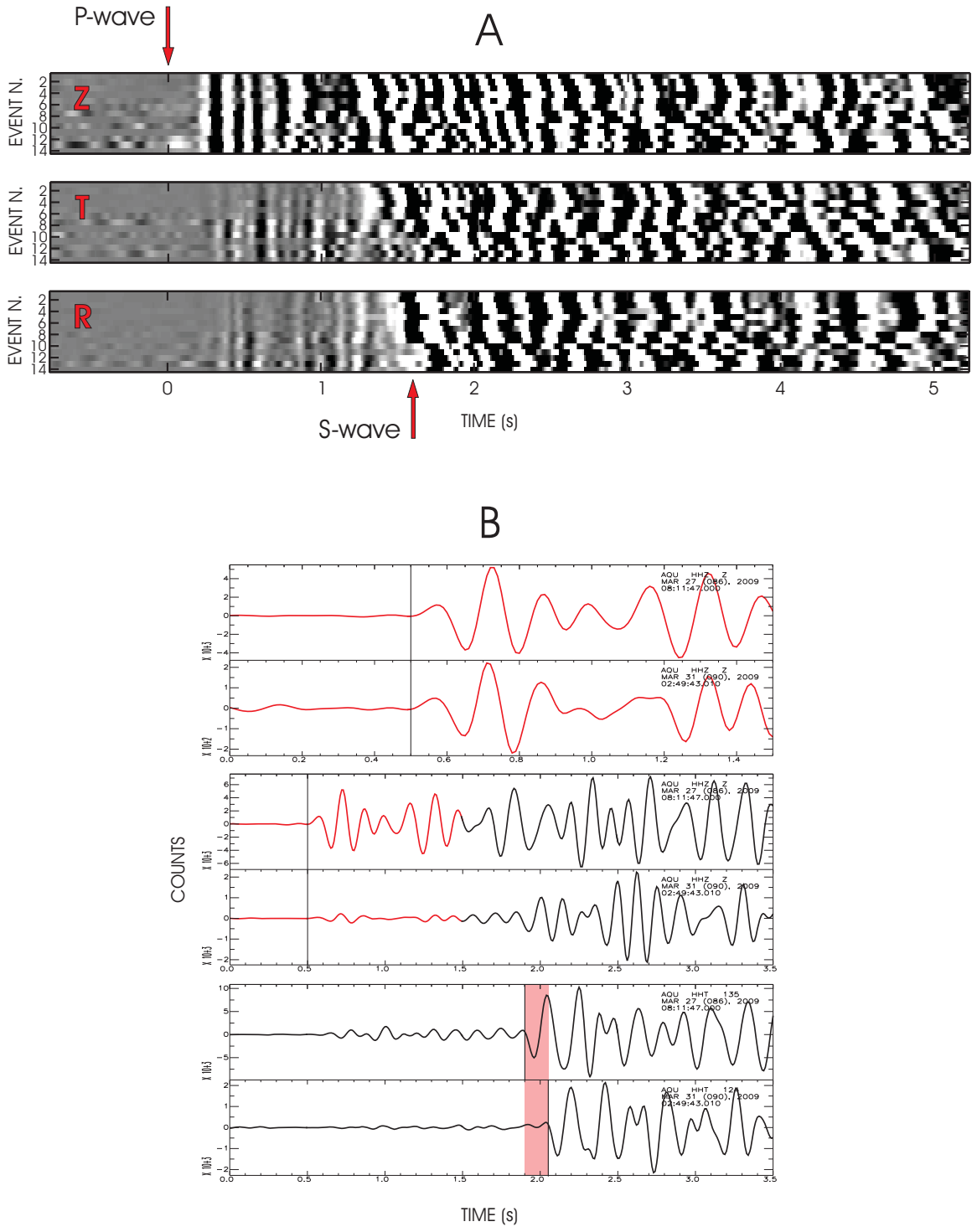

Figure DR2. Variation of the S – P arrival time for events occurring before and after March 30th. A: Gray-shaded image showing amplitudes (white shade = negative amplitude, black shade = positive amplitude) of vertical (Z), radial (R) and tangential (T) seismograms for 14 closely spaced foreshocks. Waveforms are filtered between 1 and 8 Hz. All traces are aligned on the P-wave arrival time (0 s). Vertical seismograms are cross-correlated in a time window of 0.4 s, starting from the P-wave arrivals. Traces of

events with cross-correlation > 0.8 on vertical are shown. Events are numbered in chronological order. Events occurred after March 30th (from 10 to 14) clearly display a delayed S-wave arrival. B: Comparison between highly correlated vertical (middle panel) and tangential (bottom panel) seismograms for a couple of closely spaced events occurred before and after March 30th. Waveforms are aligned on the P-wave arrival. The two seconds around the P-wave arrival (red trace in the middle panel) are magnified in the top panel to highlight the waveforms similarity. Pink shaded area on tangential seismograms marks the delay in the S-wave arrival for the event occurred after March 30th.

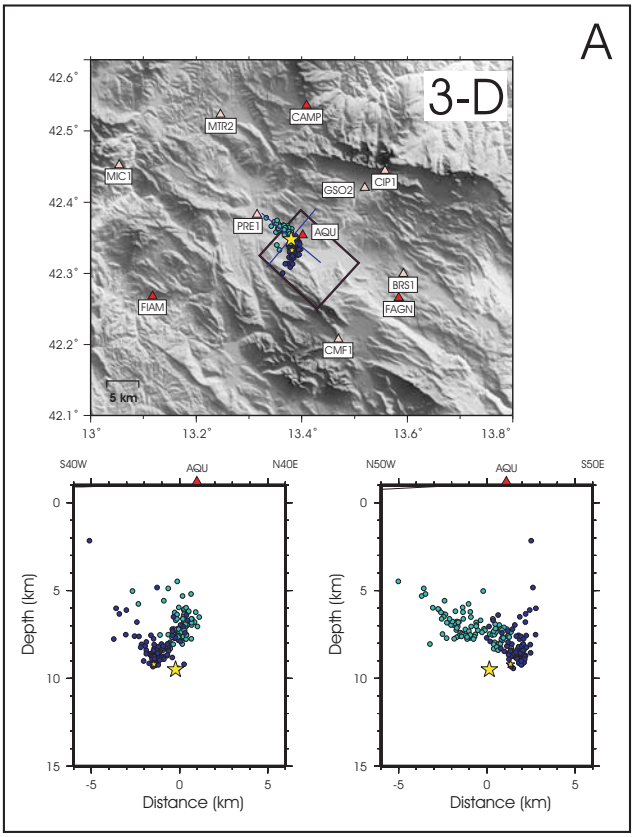
A
3-D
MTR2
CAMP
MIC1
GSO2
CIP1
PRE1
AQU
BRS1
FIAM
FAGN
CMF1
5 km
42.6°
42.5°
42.4°
42.3°
42.2°
42.1°
13°
13.2°
13.4°
13.6°
13.8°
S40W
AQU
N40E
N50W
S50E
Depth (km)
Distance (km)

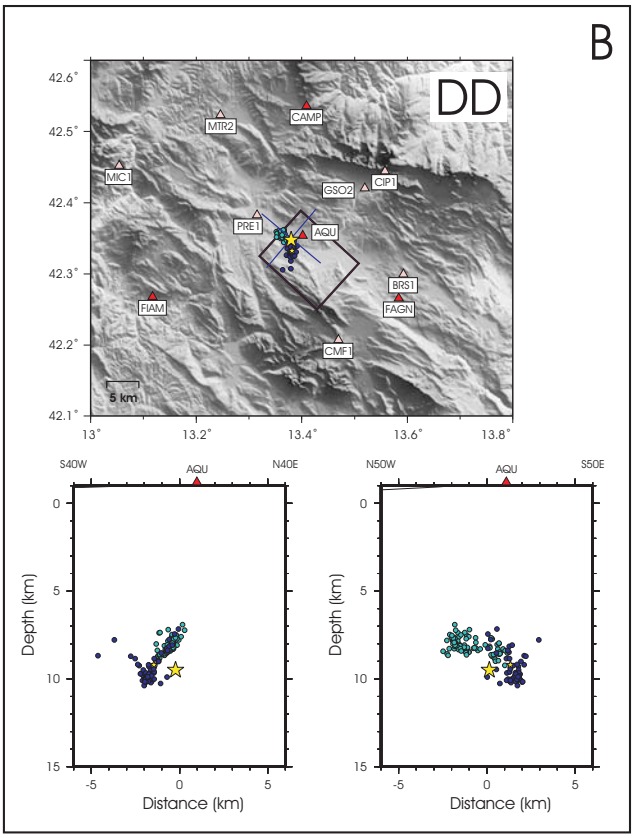
B
DD
MTR2
CAMP
MIC1
GSO2
CIP1
PRE1
AQU
BRS1
FIAM
FAGN
CMF1
5 km
42.6°
42.5°
42.4°
42.3°
42.2°
42.1°
13°
13.2°
13.4°
13.6°
13.8°
S40W
AQU
N40E
N50W
S50E
Depth (km)
Distance (km)

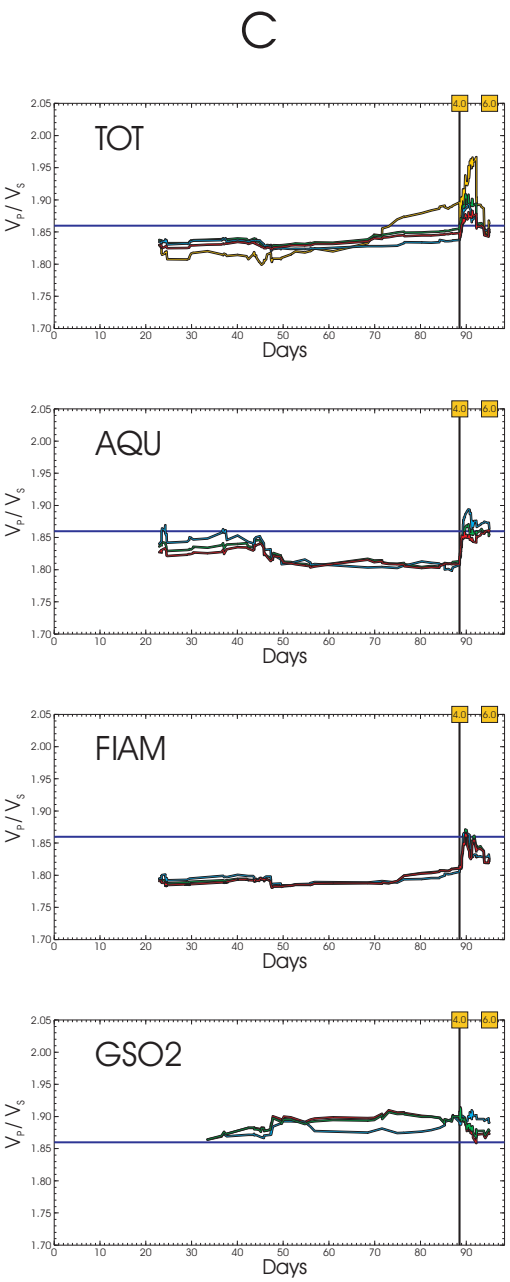
C
TOT
AQU
FIAM
GSO2
V_P / V_S
Days
4.0
6.0

Figure DR3

Figure DR3. A: Hypocenters of the foreshocks computed from the 3-D location procedure. B: Hypocenters of the foreshocks computed through the double differences code HypoDD (Waldhauser and Ellsworth, 2000). Symbols in both the maps and the cross sections are the same as in Fig. 1 of the paper. In all the maps and cross sections the location of the April 6th 2009 main shock hypocenter (larger yellow star) is kept fixed for comparison to that of Fig. 1of the paper. C: Comparison among trends of the mean V_P/V_S values at the whole set of stations, TOT, and at stations AQU, FIAM, and GSO2, calculated on running windows of 20 samples with one sample step. The green lines in each panel is the mean values interpolating function shown in the Fig. 2 of the paper. The yellow line on TOT panel is the interpolating function of the V_P/V_S mean values computed through the Hypoellipse method (Lahr, 1980). The red line on each panel is the interpolating function of the V_P/V_S mean values computed for earthquakes localized in a 3-D, P and S waves, velocity model (Di Stefano et al., in prep). The blue line on each panel is the interpolating function of the V_P/V_S mean values computed for earthquakes localized through the double difference method (Waldhauser and Ellsworth, 2000).

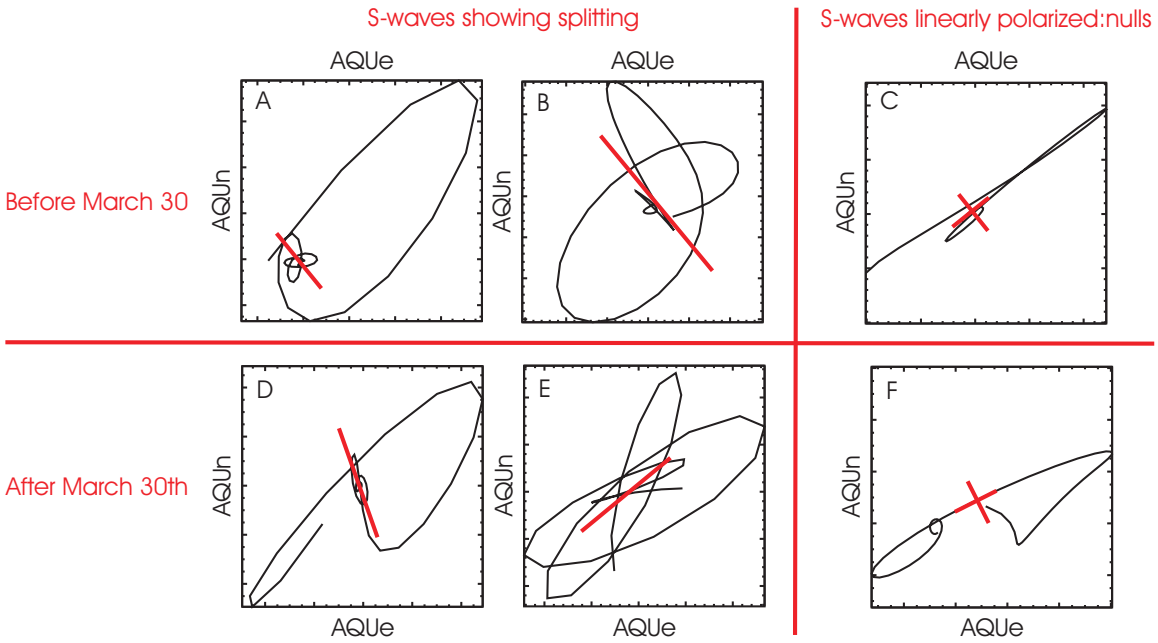

Figure DR4. Examples of particle motion of first S-wave arrival on the horizontal plane, at station AQU (waveforms are filtered between 1 and 10 Hz). On panel A, B, D, and E, the red bar is parallel to the fast splitting direction and its length is proportional to the delay time. On panels C, and F the red cross represents the S-wave linear polarization direction and the corresponding perpendicular direction (possible fast and slow splitting waves directions of the anisotropic medium). A: Split S-wave from the January-February epoch: fast direction (φ) at about N140E, small delay time (δt), elliptical particle motion on the horizontal plane. B: Split S-wave from the second half of March epoch: φ at about

N140E, large δt, cross particle motion on the horizontal plane. C: S-wave particle motion showing linear polarization found on recordings before March 30th: polarization direction at about N50E. D: Split S-wave after March 30th: easy detectable φ at about N160E, quite large δt. E: Split S-wave after March 30th: flipped φ at about N50E, small δt (elliptical particle motion). F: S-wave particle motion showing linear polarization found on recordings after March 30th: polarization direction at about N70E.

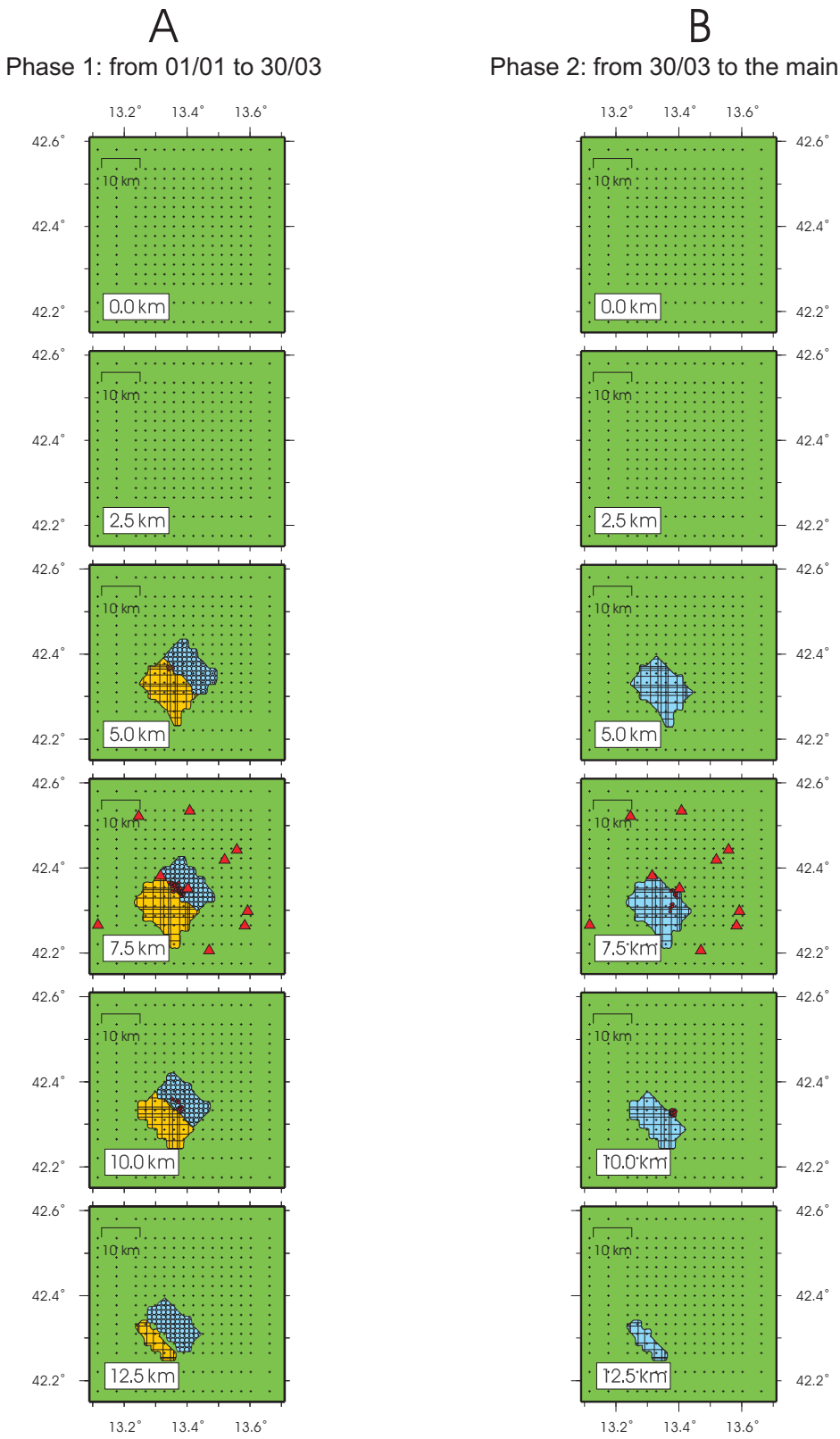

Figure DR5. Horizontal layers of the two phases V_P/V_S model at different depth. A: First phase; B: Second phase. On the both phases model layers the green color indicates the

unperturbed volume of the model (see Table DR1); orange and light blue filled areas represent the P- and S-wave velocity anomalies, respectively (see Fig. 4 of the paper for velocity anomaly values); red dots are the hypocenters of the foreshocks; red triangles are the seismic stations, projected at 7.5 km depth to highlight the station location with respect to the synthetic anomalies.

TABLE DR1. P-WAVE VELOCITY MODEL AND V_P/V_S USED TO LOCATE THE FORESHOCKS.

Depth of the layer top (km)	V_P (km/s)	V_P/V_S
0	5.48	1.86
4	6.16	1.86
8	6.45	1.86
12	6.87	1.86
16	7.06	1.86
34	8.0	1.86

Note: the 1D model is from Chiarabba et al., 2009

TABLE DR2. STATISTICAL ATTRIBUTES OF THE V_P/V_S POPULATIONS BEFORE AND AFTER THE TIME OF OCCURRENCE OF THE ML = 4 FORESHOCK, ON MARCH 30TH.

	Before March 30th				After March 30th			
	N° of measurements (n)	Mean V_P/V_S	Standard deviation (σ)	95% confidence interval	N° of measurements (n)	Mean V_P/V_S	Standard deviation (σ)	95% confidence interval
TOT	103	1.846	0.021	1.842-1.850	85	1.874	0.046	1.865-1.884
AQU	102	1.827	0.045	1.818-1.836	85	1.854	0.041	1.845-1.863
FIAM	95	1.795	0.028	1.790-1.801	72	1.840	0.079	1.821-1.858
GSO2	65	1.889	0.066	1.873-1.905	61	1.884	0.056	1.870-1.898

Note: The 95% confidence interval is defined as $mean(V_P/V_S) \pm \left(\frac{\sigma}{\sqrt{n}} * 1.96\right)$, where $\left(\frac{\sigma}{\sqrt{n}}\right)$ is the standard error of the mean (SE), and 1.96 is the .975 quantile of the normal distribution.